

Machine learning suggests climate and seasonal definitions should change under global warming

Milton Speer^{1,*}, Lance Leslie¹

Academic Editor: Supriyo Chakraborty

Abstract

Extreme and unseasonal temperature and precipitation events have increased worldwide. The greater frequency and variability of floods, heatwaves, and droughts challenge traditional definitions of climate periods as 30-year means. Machine learning (ML) studies, focusing on southern Australia, identified the dominant attributes of these precipitation and temperature events. The attributes are both local and remote climate drivers, amplified by global warming. Their impacts include longer, hotter warm seasons and shorter, drier wet seasons in Australia's southern Mediterranean climate regions. In contrast, flooding has increased in coastal eastern Australia. The poleward contraction of mid-latitude westerly winds is a readily identifiable contributor. Improvements in climate models are expected to more accurately predict future phases of climate drivers. Because global warming is not uniform across the Earth's surface, the revised definitions of climate will vary by region. In this work, we chose one clear example that supports the need for re-considering climate periods.

Keywords: *floods, droughts, extremes, southern Australian climate, polar vortex, machine learning*

Citation: Speer M, Leslie L. Machine learning suggests climate and seasonal definitions should change under global warming. *Academia Environmental Sciences and Sustainability* 2024;1. <https://doi.org/10.20935/AcadEnvSci7419>

1. Introduction

Since 2019, the term “unprecedented” has been used repetitively as frequent heatwaves, droughts, and associated bushfires have taken many lives and destroyed much property in southern and eastern Australia. Globally, in 2023 and 2024, long-lasting, deadly heatwaves struck South and East Asia, the United States, southern West Africa, and parts of Central and South America. Devastating floods that occurred in numerous countries also have been described as “unprecedented.”

In this study, we focus on southern coastal Australia, which has suffered extreme heatwaves and droughts. Machine learning (ML) studies by the authors revealed an increased frequency of unseasonable heatwaves and droughts. These findings have raised questions concerning the applicability of existing definitions of climatological standard norms, which have implemented averaging over 30 consecutive years, as defined by the World Meteorological Organization (WMO) [1].

Worldwide, extreme and record temperature and rainfall events have increased markedly in the past two decades, causing a heavy human and economic toll. Between 1980 and 1999, 4,212 disasters linked to natural hazards were observed worldwide, claiming approximately 1.19 million lives and affecting 3.25 billion people, resulting in economic losses of approximately US\$1.63 trillion [2]. However, between 2000 and 2019, the major natural disaster events almost doubled, to 7,348, claiming 1.23 million lives and affecting 4.2 billion people (many on more than one occasion).

The global economic cost also doubled, increasing to US\$2.97 trillion [2]. Much of the increased toll is explained by increased climate-related disasters, including extreme weather events. These increased from 3,656 climate-related events in the 1980–1999 period to 6,681 climate-related disasters in the 2000–2019 period [2]. Floods and storms were the most prevalent events, and the annual number of major floods more than doubled from 1,389 to 3,254 in the past two decades worldwide [2].

Recently, the climatological standard normals were challenged over their applicability to temperature and precipitation temporal patterns in New Zealand [3]. Srinivasan et al. highlight how fixed-period temperature and precipitation normals do not reflect the reality that climate states are increasingly influenced by decadal variability, during the recent accelerated global warming (GW) period since the early to middle 1990s [3].

The examples from coastal southern Australia highlight the influence of the recent poleward contraction of the Antarctic Polar Vortex (APV) and, consequently, the Southern Hemisphere (SH) mid-latitude westerly wind belt. This critical shift was revealed by ML to be due to GW, together with its complex interactions with local and remote climate drivers [4]. Extremes in precipitation amounts have resulted in large monthly and seasonal variability and, in some cases, significant changes in their means. However, GW often amplifies or diminishes the impacts of multiple climate driver phases within a quasi-decadal period [4].

¹School of Mathematical and Physical Sciences, Faculty of Science, University of Technology Sydney, Sydney, NSW 2007, Australia.

*email: milton.speer@uts.edu.au

thereby resulting in a reduction of information when averaged over the traditional period of 30 consecutive years. It is more appropriate now to employ the available WMO averages in the form of the mean of monthly values of climatological data, which can be monthly means or totals, over any specified time period [5]. In addition, the WMO's use of period averages, which are averages of climatological data computed for any period of at least 10 years, would also be highly valuable [5].

2. The role of the Antarctic Polar Vortex

The APV is a stratospheric wind pattern that extends down to the troposphere and is caused by the temperature difference between the cold pole and the warm region of the lower latitudes. The APV has a very consistent, elongated, average seasonal and annual shape owing to the lack of mountains in the mid-latitudes of the SH in contrast to the Northern Hemisphere (NH), where the continents of Europe/Asia and North America account for much of the observed waviness in the APV.

In recent decades, the APV has strengthened and contracted poleward from the high mid-latitudes, noticeably in the cool (wet) season in Australia/New Zealand longitudes, by about 5° latitude [6]. Synoptically, it is manifested as anomalous low pressure in South American longitudes near Antarctica and anomalous high pressure in the mid-latitudes of Australian longitudes. Previously, the polar jet was located further north in the mid-latitudes and low-pressure systems and interacted more dynamically with the branches of the Subtropical Jet Stream (STJ) in the region of the upper troposphere over Australia (**Figure 1**).

Consequently, some SH Mediterranean climate regimes, including those in southern coastal Australia, have experienced dramatic reductions in their cool (wet) season rainfall means. Notably, Southwestern Australia has experienced a devastating decline in cool (wet) season rainfall of approximately 30% since 1970, particularly over the past two decades (**Figure 2a**) [7]. The decrease in rainfall has been exacerbated by increasing warm (dry) maximum temperatures (TMax) and mean temperatures over the same periods (**Figure 2b**) [8]. The impact of decreasing rainfall and increasing maximum and mean temperatures on available water supply, agriculture, and the natural environment has been acute, especially during the recent drought periods 2017–2020 and 2023–2024.

2.1. Southern versus eastern Australian coastal impacts

During the Australian cool (wet) season from May to October, as defined in [4], there are contrasting recent impacts on the southern coast compared to the east coast. Two multi-year La Niña phases (2010–2012 and 2020–2022) have impacted the eastern half of Australia and resulted in flood-producing rains, causing loss of life and infrastructure. In these La Niña phases, there were persistent, moisture-laden, onshore winds over the east coast. During the 2020–2022 La Niña, the moisture was present not only in spring and summer but also during the cool (wet) season.

However, over southern coastal Australia, the mid-latitude westerly winds that typically produce rainfall during the cool season were located well south of the Australia, resulting in the recent drought of 2017–2019 [9] and flash drought of 2023–2024 [10]. This confirms rainfall changes over Southwestern Australia and

their association to the Southern Annular Mode (SAM) and El Niño Southern Oscillation (ENSO) described in [11].

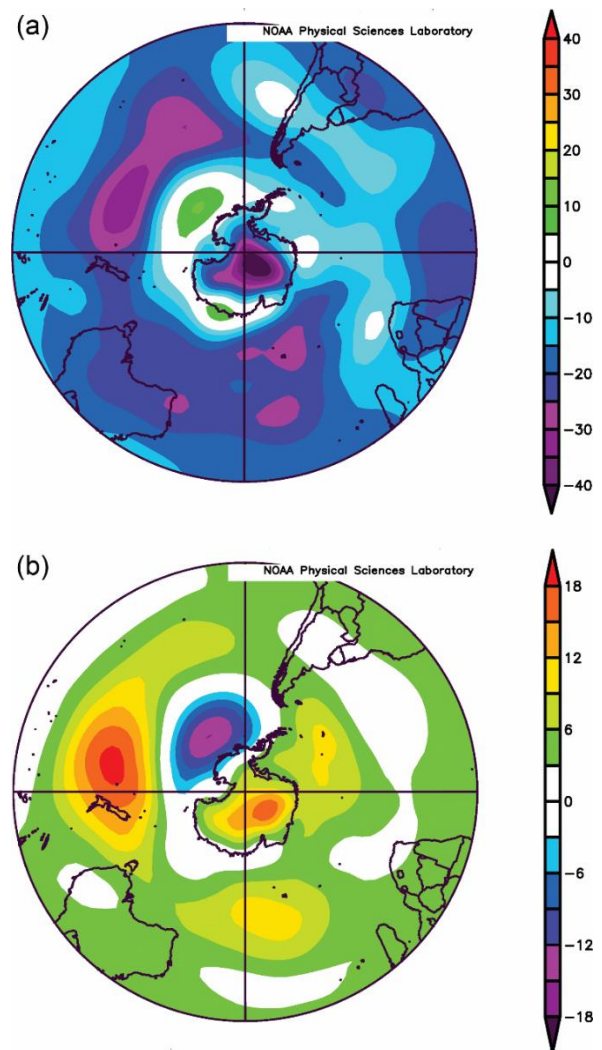


Figure 1 • (a) National Centers for Environmental Prediction (NCEP)/National Center for Atmospheric Research (NCAR) reanalysis derived 300 hPa negative gph composite anomaly from April to September in 1970–1996 (1991–2020 climatology) around the SH mid-latitudes, indicating favored areas for low-pressure rain-bearing systems; (b) NCEP/NCAR reanalysis derived 300 hPa positive gph composite anomaly from April to September in 1997–2023 (1991–2020 climatology) around the SH mid-latitudes and weakened negative anomalies around Antarctica, indicating a poleward contraction of the westerly wind regime that supports low-pressure rain-bearing systems.

2.2. Machine Learning shows how climate drivers impact Australia's southern coastal regions

ML studies focusing on both southwest and southeast coastal Australia revealed that the amplification attributes of the observed rainfall and temperature patterns are the same. Unsurprisingly, the SAM has been a dominant attribute for precipitation deficits in recent decades in the southern coastal Australian region. Negative SAM in South American longitudes, owing to the strong APV in that region, has been rendered neutral by strong positive SAM in Australian/New Zealand longitudes. The resulting contraction poleward of mid-latitude westerly zonal winds and frontal systems has decreased cool-season precipitation in southern coastal Australia.

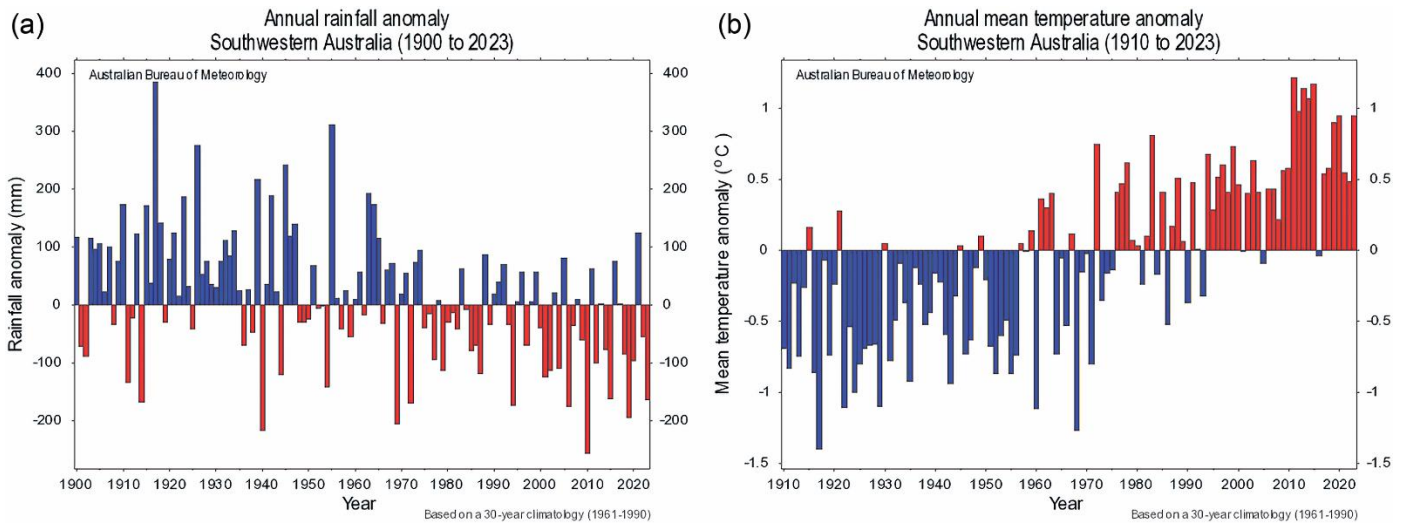


Figure 2 • (a) Annual rainfall anomaly, relative to 1961–1990, for Southwestern Australia (1900–2023) showing decline from 1970, especially from 1990. (b) Annual mean temperature anomaly for Southwestern Australia (1900–2023) showing decline from 1970, especially since the mid-1990s.

In contrast, there is increased atmospheric moisture availability from ENSO-related attributes and higher sea-surface temperatures (SSTs) off the east coast of Australia due to the presence of onshore winds. The increased atmospheric moisture has generated anomalous heavy rainfall in both warm and cool seasons in coastal and inland eastern Australia.

The reduced rainfall over southern coastal Australia has been accompanied by a notable lack of extreme rainfall. As a result of the tropospheric circulation changes described previously, southern Australian coastal areas facing the Southern Ocean lie in a rain shadow of relatively high topography from the north and east, compared to the rest of the continent. Predominantly easterly winds in Southwestern Australia are dry as they are far from any ocean moisture source that affects the east coast and too far south from a regular, northern moisture source.

3. Machine learning techniques employed

The ML techniques employed in this study for both TMax and precipitation include a correlation-based feature selection with greedy hill climbing, augmented with a backtracking facility (CfsBF) [12], and wrapper subset evaluation [13] applied to various classifiers: linear regression (LRBF), neural network (NNBF), support vector regression (SVRBF), and random forest (RFBF). A second group of techniques used classifier subset selection (CS) [14] with each of the classifiers (LRCS, NNCS, SVRCS, RFCS). The final attribute evaluator was a CS using the same evaluators, with a technique applied to the attribute subsets (LRGr, NNGr, SVRGr, RFGr), described in [15].

4. Perth maximum temperature attribute selection

Perth is a large, representative city for southwest coastal Australia. Perth has a Mediterranean climate, with hot, dry, warm

seasons (November–April) and wet cool seasons (May–October). Importantly, Perth has a long, continuous data record of daily and monthly temperature and precipitation. The known climate drivers are the global temperature time series and time series of climate indices such as the Dipole Mode Index (DMI), Southern Oscillation Index (SOI), Niño 3, Niño 4, Pacific Decadal Oscillation (PDO), SAM, Atlantic Meridional Oscillation (AMO), North Pacific Index (NPI), and Interdecadal Pacific Oscillation (IPO) [16].

It is well known that most heat waves across southwest coastal Australia occur under prolonged strong dry easterly winds [17]. The impact of climate change was determined from permutation testing of mean maximum temperature (TMax) differences between the 20-year periods 1979–1998 and 1999–2018. Attribution employed a set of four ML techniques: linear regression (LR) [18], support vector regression (SVR) [19], artificial neural network (NN) [20], and random forest (RF) [21]. Data for the 1910–1981 period were used to determine possible attributes.

For the Perth maximum temperature (TMax) time series, the LR model that performed best contained the attributes GlobalT (GT), Niño 4, and DMI (or IOD), as shown in **Table 1**. NN uses the same attributes as LR, whereas SVR uses GT, PDO, and DMI. RF uses GT and DMI. For the precipitation predictions, LR uses NPI, SOI, and SAM; NN uses SOI and SAM; SVM uses IPO, SOI, SAM, Niño 4×SAM, and DMI×SAM; and RF uses PDO and SAM, as shown in **Table 2**. The six most dominant attributes for TMax and precipitation predictions evaluated in all methods are shown in **Tables 1** and **2** [16]. By far, the most dominant attribute for Perth maximum temperature prediction is GT, as given in **Table 1**, followed by DMI, and then PDO, AMO, NPI, and SAM. No combinations of climate drivers, except Niño 4, appear in more than 30% of the folds.

Table 1 • Attribute selection for 13 different methods for maximum temperature prediction in Perth

| Attribute/method | Cfs | LR | NN | SVR | RF | LR | NN | SVR | RF | LR | NN | SVR | RF | Mean |
|------------------|-----|------|------|------|------|------|------|------|------|------|------|------|------|------|
| | BF | BF | BF | BF | BF | CS | CS | CS | CS | Gr | Gr | Gr | Gr | |
| GT | 100 | 100 | 100 | 100 | 100 | 100 | 100 | 100 | 100 | 100 | 100 | 100 | 100 | 100 |
| NPI | 0 | 0 | 0 | 30 | 70 | 10 | 90 | 70 | 90 | 0 | 0 | 30 | 70 | 35.4 |
| AMO | 0 | 20 | 20 | 0 | 80 | 40 | 100 | 80 | 50 | 20 | 10 | 10 | 70 | 38.5 |
| PDO | 0 | 30 | 30 | 60 | 10 | 90 | 80 | 80 | 0 | 30 | 30 | 50 | 10 | 39.2 |
| DMI | 80 | 80 | 50 | 90 | 20 | 90 | 70 | 100 | 20 | 80 | 30 | 90 | 20 | 63.1 |
| SAM | 0 | 10 | 40 | 80 | 0 | 20 | 40 | 60 | 100 | 10 | 30 | 50 | 0 | 33.8 |
| Mean | 15 | 16.5 | 18 | 30.5 | 18.5 | 38 | 62 | 74 | 25 | 15.5 | 15 | 24 | 18 | |
| Standard Dev. | 30 | 29.4 | 24.8 | 30.9 | 30.8 | 39.2 | 21.2 | 22.6 | 35.5 | 28.7 | 23.2 | 30.5 | 29.7 | |

The percentage of folds selecting the attribute is shown for each of the 13 machine learning methods (columns 2–14). Statistics (mean, standard deviation) for each column are shown. The mean percentage of folds for each attribute is shown in column 15. Cfs, correlation-based feature selection; BF, backtracking facility; LR, linear regression; NN, neural network; SVR, support vector regression; RF, random forest; CS, classifier subset selection; GT, GlobalT; NPI, North Pacific Index; AMO, Atlantic Meridional Oscillation; PDO, Pacific Decadal Oscillation; DMI, Dipole Mode Index; SAM, Southern Annular Mode.

Table 2 • Attribute selection for 13 different methods for precipitation prediction in Perth

| Attribute/method | Cfs | LR | NN | SVR | RF | LR | NN | SVR | RF | LR | NN | SVR | RF | Mean |
|------------------|------|------|------|------|------|------|------|------|------|------|------|------|------|------|
| | BF | BF | BF | BF | BF | CS | CS | CS | CS | Gr | Gr | Gr | Gr | |
| NPI | 0 | 20 | 0 | 10 | 0 | 90 | 100 | 90 | 0 | 90 | 30 | 70 | 0 | 38.5 |
| Niño 3 | 0 | 0 | 10 | 30 | 90 | 10 | 60 | 80 | 90 | 0 | 30 | 40 | 50 | 37.7 |
| SOI | 70 | 90 | 50 | 100 | 20 | 100 | 100 | 100 | 20 | 100 | 90 | 100 | 30 | 74.6 |
| SAM | 100 | 80 | 80 | 100 | 90 | 100 | 100 | 100 | 90 | 100 | 90 | 100 | 90 | 93.8 |
| Niño 4×SAM | 0 | 10 | 10 | 10 | 50 | 30 | 80 | 80 | 50 | 30 | 50 | 60 | 10 | 36.2 |
| DMI×SAM | 0 | 0 | 20 | 0 | 10 | 50 | 100 | 90 | 10 | 50 | 60 | 60 | 0 | 34.6 |
| Mean | 26.7 | 12.9 | 13.3 | 20.5 | 24.3 | 21.4 | 86.2 | 69.0 | 24.3 | 20.5 | 37.6 | 44.3 | 15.7 | |
| Standard Dev. | 39.9 | 25.5 | 24.8 | 34.6 | 28.4 | 34.5 | 14.0 | 21.7 | 28.4 | 35.0 | 24.9 | 27.3 | 21.8 | |

The percentage of folds selecting the attribute is shown for each of the 13 machine learning methods (columns 2–14). Statistics (mean, standard deviation) for each column are shown. The mean percentage of folds for each attribute is shown in column 15. Cfs, correlation-based feature selection; BF, backtracking facility; LR, linear regression; NN, neural network; SVR, support vector regression; RF, random forest; CS, classifier subset selection; NPI, North Pacific Index; SOI, Southern Oscillation Index; SAM, Southern Annular Mode; DMI, Dipole Mode Index.

5. Perth precipitation attribute selection

The precipitation analysis (**Table 2**) used the same feature selection techniques as for temperature, with sea surface temperature anomalies near Perth (NPI) being an additional potential attribute. The six most relevant Perth precipitation attributes selected by the ML techniques are shown in **Table 2**. By far, the most dominant attribute is SAM, which appears in over 90% of the folds. SAM also appears in combination with Niño 4 and DMI. Finally, NPI, Niño 3, and SOI are the next three most prominent attributes [16].

6. Conclusions

In recent decades, there has been a glaring disconnect between the current definition of climate periods as the means of 30 consecutive years and the more appropriate means of decadal or shorter periods. It is generally known now that GW and climate impacts have accelerated since the 1990s. As a result, global climate regimes now are increasingly being driven by GW, modulated by the phases of climate drivers relevant to the location of interest. Using the “Mediterranean climate” of

southern coastal Australia as an example, we demonstrate how the means and variances of maximum temperature and precipitation time series can change dramatically on interdecadal, or even shorter, temporal spans. These rapid temporal changes render the means of 30 consecutive years as no longer being representative of climate periods. The coastal and near-coastal regions of southern Australia under threat in future. If the three largest southern coastal cities of Perth, Adelaide, and Melbourne are included, the region accounts for over 35% of Australia’s total population, in addition to providing fertile land for grazing, farming, energy production, and export and import facilities. Finally, our recent work has emphasized the need for a combined statistical model approach to climate prediction [10, 22]. Climate models are needed to predict the future phases of the climate drivers for which ML techniques can be used to project the future climate states. A new type of hybrid ML–General Circulation Model (GCM), termed “Neural GCMs,” has been developed for weather and climate prediction [23]. It has shown promise, and hopefully this generation of GCMs can incorporate ML techniques that consider nonstationary time series such as temperature and precipitation, which have become nonstationary due to

accelerated GW in recent decades. GW is not uniform across the Earth's surface, and hence the revised definitions of climate would vary by region. However, there are numerous examples of the need for a changed definition of a regional climate. We chose one very clear supporting example in our study.

Acknowledgments

The authors acknowledge the support of the School of Mathematical and Physical Sciences, University of Technology Sydney for encouraging this research.

Funding

The authors declare no financial support for the research, authorship, or publication of this article.

Author contributions

Conceptualization, M.S. and L.L.; methodology, L.L. and M.S.; software, L.L. and M.S.; validation, L.L. and M.S.; formal analysis, M.S.; investigation, M.S.; resources, L.L.; data curation, M.S.; writing—original draft preparation, M.S.; writing—review and editing, L.L.; visualization, M.S. and L.L.; project administration, M.S. Both authors have read and agreed to the published version of the manuscript.

Conflict of interest

The authors declare no conflict of interest.

Data availability statement

Data supporting these findings are available within the article, at <https://doi.org/10.20935/AcadEnvSci7419>, or upon request.

Institutional review board statement

Not applicable.

Informed consent statement

Informed consent was obtained from all subjects involved in the study.

Additional information

Received: 2024-07-24

Accepted: 2024-11-08

Published: 2024-11-21

Academia Environmental Sciences and Sustainability papers should be cited as *Academia Environmental Sciences and Sustainability 2024*, ISSN 2997-6006, <https://doi.org/10.20935/AcadEnvSci7419>. The journal's official abbreviation is *Acad. Env. Sci. Sust.*

Publisher's note

Academia.edu Journals stays neutral with regard to jurisdictional claims in published maps and institutional affiliations. All claims expressed in this article are solely those of the authors and do not necessarily represent those of their affiliated organizations, or those of the publisher, the editors, and the reviewers. Any product that may be evaluated in this article, or claim that may be made by its manufacturer, is not guaranteed or endorsed by the publisher.

Copyright

© 2024 copyright by the authors. This article is an open access article distributed under the terms and conditions of the Creative Commons Attribution (CC BY) license (<https://creativecommons.org/licenses/by/4.0/>).

References

1. World Meteorological Organization. Climatological normals; 2020 [cited 2024 July]. Available from: <https://community.wmo.int/en/wmo-climatological-normals>
2. United Nations Office for Disaster Risk Reduction. Centre for Research on the Epidemiology of Disasters. The human cost of disasters: an overview of the last 20 years (2000–2019); 2020 [cited July 2024]. Available from: <https://www.undrr.org/publication/human-cost-disasters-overview-last-20-years-2000-2019>
3. Srinivasan R, Carey-Smith T, Wang L, Harper A, Dean S, Macara G, et al. Moving to a new normal: analysis of shifting climate normals in New Zealand. *Int J Climatol.* 2024; 44(10):1–24. doi: 10.1002/joc.8521
4. Speer M, Hartigan J, Leslie L. The machine learning attribution of quasi-decadal precipitation and temperature: extremes in Southeastern Australia during the 1971–2022 period. *Climate.* 2024;12:75. doi: 10.3390/cli12050075
5. World Meteorological Organization. The role of climatological normals in a changing climate. WMO/TD-No. 1377. WMO-No. 1203; 2007 [cited 2024 July]. Available from: <https://library.wmo.int/records/item/52499-the-role-of-climatological-normals-in-a-changing-climate?offset=45>
6. Speer MS, Leslie LM, Hartigan J. Jet stream changes over Southeast Australia during the early cool season in response to accelerated global warming. *Climate.* 2022;10:84. doi: 10.3390/cli10060084
7. Australian Bureau of Meteorology. Annual rainfall anomaly for Southwestern Australia; 2024 [cited July 2024]. Available from: http://www.bom.gov.au/cgi-bin/climate/change/timeseries.cgi?graph=rranom&area=sवास&season=0112&ave_yr=0&ave_period=6190
8. Australian Bureau of Meteorology. Annual mean temperature anomaly for Southwestern Australia; 2024 [cited July 2024]. http://www.bom.gov.au/cgi-bin/climate/change/timeseries.cgi?graph=tmean&area=sवास&season=0112&ave_yr=0&ave_period=6190
9. Devanand A, Falster GM, Gillett ZE, Hobeichi S, Holgate CM, Jin C, et al. Australia's tinderbox drought: an extreme

- natural event likely worsened by human-caused climate change. *Sci Adv.* 2024;10:eadj3460. doi: 10.1126/sciadv.adj3460
10. Speer M, Hartigan J, Leslie LM. Machine learning identification of attributes and predictors for a flash drought in Eastern Australia. *Climate.* 2024;12:49. doi: 10.3390/cli12040049
 11. Raut BA, Jakob C, Reeder MJ. Rainfall changes over Southwestern Australia and their relationship to the southern annular mode and ENSO. *J Clim.* 2014;27:5801–14. doi: 10.1175/JCLI-D-13-00773.1
 12. Hall MA. Correlation-based feature subset selection for machine learning [PhD dissertation]. Hamilton: Department of Computer Science. University of Waikato; 1998.
 13. Kohavi R, John GH. Wrappers for feature subset selection. *Artif Intell.* 1997;97(1–2):273–324. [https://doi.org/10.1016/S0004-3702\(97\)00043-X](https://doi.org/10.1016/S0004-3702(97)00043-X)
 14. Mendialdua I, Arruti A, Jauregi E, Lazkano E, Sierra B. Classifier subset selection to construct multi-classifiers by means of estimation of distribution algorithms. *Neurocomputing.* 2015;157:46–60. <https://doi.org/10.1016/j.neucom.2015.01.036>
 15. Caruana R, Freitag D. Greedy attribute selection. *Mach Learn Proc.* 1994;48:28–36. <https://doi.org/10.1016/B978-1-55860-335-6.50012-X>
 16. Richman MB, Leslie LM. Machine learning for attribution of heat and drought in Southwestern Australia. *Procedia Comput Sci.* 2020;168:3–10. doi: 10.1016/j.procs.2020.02.244
 17. Leslie LM. Numerical modeling of the summer heat low over Australia. *J Appl Meteorol.* 1980;19(4):381–7. doi: 10.1175/1520-0450(1980)019<0381:NMOTSH>2.0.CO;2
 18. Ramsey HA, Richman MB, Leslie LM. Seasonal tropical cyclone predictions using optimized combinations of ENSO regions: application to the Coral Sea basin. *J Climate.* 2014;27:8527–42. doi: 10.1175/JCLI-D-14-00017.1
 19. Richman MB, Leslie LM, Mansouri H, Trafalis TB. Data selection using support vector regression. *Adv Atmos Res.* 2014;32:277–86. doi: 10.1007/s00376-014-4072-9
 20. Pasini A, Racca P, Amendola S, Cartocci G, Cassardo C. Attribution of recent temperature behaviour reassessed by a neural network method. *Sci Rep.* 2017;7:17681. doi: 10.1038/s41598-017-18011-8
 21. Naing WYN, Htike ZZ. Forecasting of monthly temperature variations using random forests. *ARPN J Eng Appl Sci.* 2015; 10:10109–12. ISSN: 1819-6608.
 22. Speer M, Hartigan J, Leslie L. Machine learning assessment of the impact of global warming on the climate drivers of water supply to Australia’s Northern Murray-Darling Basin. *Water.* 2022;14(19):3073. doi: 10.3390/w14193073
 23. Kochkov D, Yuval J, Langmore I, Norgaard P, Smith J, Mooers G, et al. Neural general circulation models for weather and climate. *Nature.* 2024;632:1060–6. doi: 10.1038/s41586-024-07744-y